

High-power quantum cascade lasers grown by low-pressure metal organic vapor-phase epitaxy operating in continuous wave above 400 K

Cite as: Appl. Phys. Lett. **88**, 201115 (2006); <https://doi.org/10.1063/1.2203964>

Submitted: 28 December 2005 . Accepted: 14 April 2006 . Published Online: 17 May 2006

L. Diehl, D. Bour, S. Corzine, J. Zhu, G. Höfler, M. Lončar, M. Troccoli, and Federico Capasso



View Online



Export Citation

ARTICLES YOU MAY BE INTERESTED IN

[Buried heterostructure quantum cascade lasers with high continuous-wave wall plug efficiency](#)

Applied Physics Letters **91**, 071101 (2007); <https://doi.org/10.1063/1.2770768>

[1.6W high wall plug efficiency, continuous-wave room temperature quantum cascade laser emitting at 4.6 \$\mu\$ m](#)

Applied Physics Letters **92**, 111110 (2008); <https://doi.org/10.1063/1.2899630>

[Room temperature quantum cascade lasers with 27% wall plug efficiency](#)

Applied Physics Letters **98**, 181102 (2011); <https://doi.org/10.1063/1.3586773>

Lock-in Amplifiers
up to 600 MHz



High-power quantum cascade lasers grown by low-pressure metal organic vapor-phase epitaxy operating in continuous wave above 400 K

L. Diehl

*Division of Engineering and Applied Science, Cruft Laboratory 310, Harvard University,
19 Oxford Street, Cambridge, Massachusetts 02138*

D. Bour, S. Corzine, J. Zhu, and G. Höfler

Agilent Laboratories, 3500 Deer Creek Road, Palo Alto, California 94304

M. Lončar, M. Troccoli, and Federico Capasso^{a)}

*Division of Engineering and Applied Science, Cruft Laboratory 310, Harvard University,
19 Oxford Street, Cambridge, Massachusetts 02138*

(Received 28 December 2005; accepted 14 April 2006; published online 17 May 2006)

High-power quantum cascade lasers (QCLs) working in continuous wave (cw) above 400 K are presented. The material was grown by low-pressure metal organic vapor-phase epitaxy and processed into narrow buried heterostructure lasers. A cw output power of 204 mW was obtained at 300 K with an 8.38 μm wavelength, 3 mm long and 7.5 μm wide coated laser. The device operates in cw mode above 400 K, which exceeds the previous maximum cw temperature operation of QCLs by approximately 60 K. Preliminary reliability data obtained by accelerated aging tests indicate a remarkable robustness of the lasers. © 2006 American Institute of Physics.

[DOI: 10.1063/1.2203964]

It has been shown in the last few years that quantum cascade lasers (QCLs) are an ideal light source for many chemical sensing applications in the midinfrared.^{1,2} Indeed stable single mode operation, which is highly desirable for these applications can be achieved with QCLs by means of an external cavity³ or by fabricating distributed feedback lasers,⁴ for example. In addition, QCLs can work in continuous wave (cw) at temperatures above 300 K with high output power, as discussed in Refs. 4 and 5. A recent article reported a cw power of 446 mW at 292 K and a maximum temperature operation of 333 K for a 15 μm wide, 3 mm long device emitting at 6 μm .⁶ As the commercial significance of QCLs increases, the production of reliable and potentially low-cost devices becomes increasingly important. The question of whether or not high performance can be obtained from QCLs grown by metal organic vapor-phase epitaxy (MOVPE) is central since this technique is a widely established platform for the high-volume production of reliable semiconductor lasers. This question was partially answered recently by the demonstration of room temperature cw operation with lattice matched QCLs grown by MOVPE.⁷ The devices tested, which were based on a basic three quantum well active region design, worked cw up to 320 K with an output power of more than 20 mW at 300 K.

In this letter we report the fabrication of MOVPE-grown QCLs having performance comparable to the best results obtained with MBE material.⁶ The maximum collected output power from a 7.5 μm wide, 3 mm long QCL is as high as 204 mW at 300 K after the evaporation of a high-reflection (HR) coating. This device operated in continuous mode up to 400 K with more than 10 mW of output power. Note that throughout this letter, the values of the output power and the slope efficiency are not corrected for the collection efficiency of our setup, which is estimated to be 70%.

The QCLs investigated here were grown by low-pressure MOVPE in a standard reactor equipped with a

purged and pressure-balanced switching manifold and a close-spaced showerhead injector. More details about the growth can be found in Refs. 8 and 9. The active region of the samples studied is based on a double-phonon resonance design identical, except for the doping level in the injector, to the design reported by Hofstetter *et al.*¹⁰ 35 states were grown at a slow rate of 0.1 nm/s. The doping in the injector was kept low ($1 \times 10^{17} \text{ cm}^{-3}$) to limit the optical losses. The waveguide surrounding the active region consists of two InGaAs layers (thickness of 0.52 μm , Si:doping of $3 \times 10^{16} \text{ cm}^{-3}$) and two thick InP cladding layers (thickness of 3.5 μm , Si:doping of $1 \times 10^{17} \text{ cm}^{-3}$) grown at a fast rate of 0.5 nm/s. The growth sequence ended with the deposition of a plasmon-confinement layer (InP, thickness of 0.5 μm , Si:doping of $5 \times 10^{18} \text{ cm}^{-3}$) and 20 nm n^+ InGaAs capping layer.

Buried heterostructure lasers were processed using conventional fabrication techniques. Ridges with a width of either 3 or 7.5 μm were etched by a combination of wet and dry etching. Fe-doped InP was then regrown to planarize the structure, helping to decouple laterally the optical mode from the lossy metal contacts and to lower the thermal resistance of the device while minimizing leakage currents. Electrical contacts are provided by Ti/Au metallizations evaporated directly onto the n^+ InGaAs capping layer and the Fe:InP surrounding the laser ridge. An additional 5 μm thick gold layer was subsequently electroplated to further improve heat dissipation. The devices were finally mounted ridge side up onto copper blocks and wire bonded. The lasers were tested inside a Peltier-cooled box with a CaF₂ window. The temperature of the heat sink was monitored with a Si diode placed near the QCLs. The light from one facet was collected by $f/1$ optics and a calibrated thermopile detector was used to perform power measurements. The optical spectra were recorded with a Nicolet 860 Fourier transform interferometer.

Figure 1 shows the voltage and the light intensity versus current (V - I and L - I) curves of 3 mm long lasers having,

^{a)}Electronic mail: capasso@deas.harvard.edu

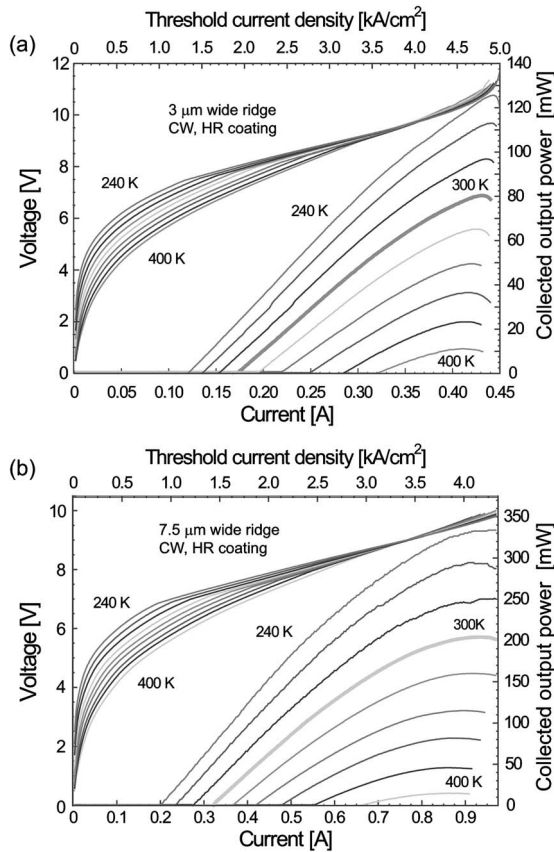


FIG. 1. cw L - I and V - I curves of HR coated 3 mm long lasers with (a) 3 μm and (b) 7.5 μm ridge widths. The heat sink temperature was varied between 240 and 400 K in steps of 20 K. The optical power data, taken from one laser facet, are not corrected for the estimated 70% collection efficiency of our setup.

respectively, 3 and 7.5 μm ridge widths. The measurements were performed with the devices operating in cw mode and at temperatures ranging from 240 to 400 K. A HR coating consisting of 200 nm Al_2O_3 and 30 nm Au was evaporated on the backfacet of both devices and nearly doubled the maximum collected output power P_{max} of both the narrow and the broad laser. The value of P_{max} , measured at room temperature with the 7.5 μm wide QCL, was indeed 115 and 204 mW before and after the deposition of the HR coating. Note that the total output power after backfacet coating should be as high as 291 mW given the estimated collection efficiency. The above improvement was accompanied by a decrease of approximately 20% of the threshold current density of both devices. From this change, an estimate of the waveguide losses was deduced and yields 8.3 and 9 cm^{-1} for the broad and the narrow laser, respectively.

A remarkable feature is that both lasers work in continuous mode at 400 K with more than 10 mW of output power. It exceeds the previous maximum cw temperature operation of QCLs by approximately 60 K.¹¹ At room temperature, the maximum collected output power reaches 80 and 204 mW with a corresponding slope efficiency dP/dI equal to 372 and 473 mW/A for the narrow and the broad laser, respectively. In a QCL, as the current is increased above threshold, an electron creates a number of photons equal to the number of stages N . It is thus appropriate to define a differential quantum efficiency *per stage* as $\eta_d = e(Nh\nu)^{-1} dP/dI$ with $h\nu$ the photon energy. Note that P in this equation is equal to the power collected from a single facet of a HR coated laser.

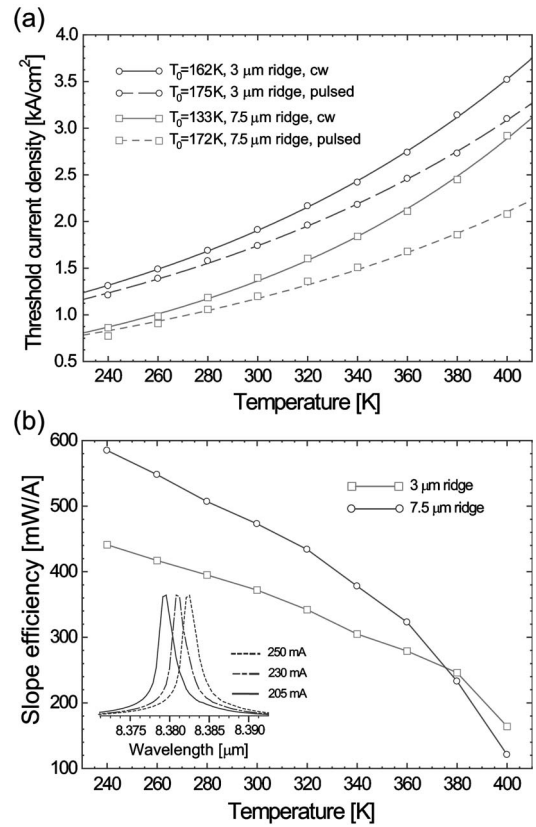


FIG. 2. (a) Threshold current density as a function of heat sink temperature for the HR coated, 3 mm long lasers with 3 μm (circles) and 7.5 μm (squares) ridge width in pulsed (dashed line) and cw modes (solid line). The experimental points (open symbols) are fitted by the expression $j_{\text{th}} = j_0 e^{T/T_0}$. (b) Slope efficiency vs temperature deduced from the L - I curves shown in Fig. 1(b) close to threshold. Inset: high-resolution cw spectra as a function of injection current measured with the 3 μm wide QCL without HR coating at a constant temperature of 300 K.

If the 70% collection efficiency of our setup is taken into account, η_d yields, in the case of the HR coated 7.5 μm wide QCL, 13.1% and 3.32% at, respectively, 300 and 400 K. With these numbers and the estimate of the internal loss $\alpha_{\text{waveguide}}$, the internal quantum efficiency (per stage) η_i can be found from the standard formula $\eta_i = \eta_d(1 + \alpha_{\text{waveguide}}/\alpha_{\text{mirror}})$, where $\alpha_{\text{mirror}} = 2.15 \text{ cm}^{-1}$ is the mirror loss. When $\eta_d = 13.1\%$, the internal quantum efficiency is about 63.7%, which is comparable to standard edge-emitting diode lasers.

The value of the threshold current density j_{th} measured in cw and pulsed mode (1.5% duty cycle, 80 KHz repetition rate) is plotted as a function of temperature in Fig. 2(a). The pulsed threshold current of the narrow device is approximately 44% larger than the value found for the broad laser. This percentage difference is essentially constant over the entire temperature range and is explained by the reduction of the overlap of the optical mode with the gain medium as the stripe width narrows. j_{th} is indeed proportional to the total optical losses divided by the overlap factor Γ . Using the waveguide loss mentioned earlier in the text and the values of Γ calculated with a two-dimensional (2D) beam-propagation modeling program (38% and 55% for the narrow and the broad QCL, respectively), j_{th} is found to be 54% larger for the 3 μm wide lasers compared to the broad device, in good agreement with the experimental data. The cw threshold current densities of the 3 μm wide laser are 1.9 kA/cm^2 at room temperature and 3.5 kA/cm^2 at 400 K.

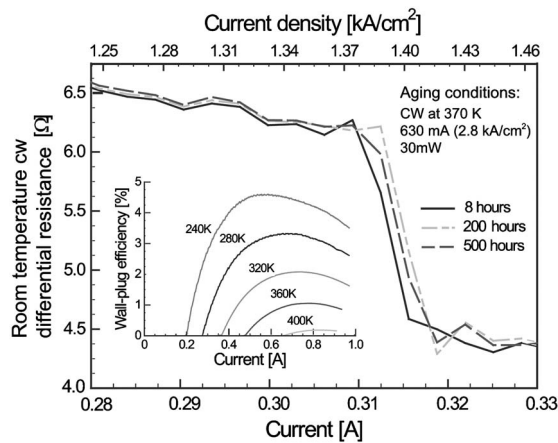


FIG. 3. Room temperature cw differential resistance of the $7.5 \mu\text{m}$ HR coated device as a function of current after 8, 200, and 500 h of cw operation at 370 K. The discontinuity indicates the position of the threshold current. Inset: wall-plug efficiency as a function of current for temperatures ranging from 240 to 400 K.

As in pulsed mode, the corresponding values for the wider laser are lower (1.39 kA/cm^2 at 300 K and still less than 3 kA/cm^2 at 400 K).

It is apparent from Figs. 1 and 2(a) that the $7.5 \mu\text{m}$ wide ridge is the most sensitive of the two samples with respect to temperature changes. The characteristic temperature T_0 , which describes phenomenologically the increase of j_{th} with temperature, has a similar value in pulsed mode for both the narrow and the broad laser. A much larger T_0 is found, however, in continuous mode for the $3 \mu\text{m}$ wide device, which confirms that a narrow stripe width leads to performance less sensitive to temperature. This conclusion is supported by Fig. 2(b), in which the slope efficiency is plotted as a function of temperature. The value of dP/dI clearly decreases faster for the device with a broader ridge as the temperature increases and above 380 K, the slope efficiency of the narrowest sample even becomes larger. The better heat removal capability of the narrow stripe laser translates into a higher value of the thermal conductance $G_{\text{th}} = (R_{\text{th}}A)^{-1}$. Here A is the device area and R_{th} (10.84 and 11.79 K/W for the 3 and $7.5 \mu\text{m}$ device at 300 K) is the thermal resistance which can be determined from the threshold current density versus temperature curves shown in Fig. 2(b).⁶ At 300 K, the thermal conductance yields 942 and 394 W/Kcm^2 for, respectively, the narrow and the broad device. Note that the G_{th} ratio of 2.39 is very close to the stripe width ratio of 2.5. The larger value of G_{th} found for the $3 \mu\text{m}$ stripe is understandable as the ratio of volume to area is more favorable in terms of heat dissipation for narrower ridges. Similar conclusions were reached in previous studies.¹²

The inset of Fig. 2(b) shows typical emission spectra obtained above threshold with the devices investigated in the present letter. The different curves were measured at 300 K with a $3 \mu\text{m}$ wide laser operating in continuous mode. The emission wavelength is $8.38 \mu\text{m}$ and little shorter than the one of Refs. 10. Note that the optical spectra broadened and showed lasing in many modes when the devices were pumped at current densities at least 30% above j_{th} . A detailed study of this phenomenon will be published elsewhere. The wall-plug efficiency, defined as the total optical output power divided by the electrical input power, is shown in the inset of Fig. 3 for the HR coated $7.5 \mu\text{m}$ wide device. The I - V and L - I curves presented in Fig. 1(b) were used in the calcula-

tions. The wall-plug efficiency is as high as 4.6% at 240 K and 0.18% at 400 K. Given the estimated collection efficiency of our setup, these values should be approximately a factor of 1/0.7 larger.

Preliminary results obtained in the context of accelerated aging measurements are also promising. The $7.5 \mu\text{m}$ wide laser, whose performance is described in this letter was operated for long periods of time in cw at 370 K and a constant current of 630 mA, corresponding to an output power of 30 mW and a current density of 2.8 kA/cm^2 . At regular intervals, the cw L - I and I - V curves were measured at 300 K. After more than 500 h, only negligible variations in the threshold current and slope efficiency were observed. Figure 3 shows, for example, the differential resistance of the device, deduced from the I - V curves measured at room temperature after 8, 200, and 500 h of cw operation at 370 K. The threshold current corresponds to the discontinuity in each of the traces. It varies between curves by less than 2 mA. This change (approximately 0.6%) is insignificant as it is comparable to the measurement error. The latter is equal to 3 mA and is due to the fact that the heat sink temperature is only controlled within 0.2 K. Note that the box in which the laser was mounted was not purged with dry air or nitrogen. A more detailed description of the results will be given elsewhere.

In conclusion, $8.38 \mu\text{m}$ wavelength, HR coated QC lasers grown by low-pressure MOVPE and processed into narrow buried heterostructures were operated in cw mode up to 400 K. High cw output powers as high as 204 mW at room temperature and more than 10 mW at 400 K were measured. The laser characteristics reported here represent a significant improvement in the performance of MOVPE-grown QCLs.

The Harvard group acknowledges partial financial support from Agilent Technologies, from the U.S. Army Research Laboratory and the U.S. Army Research Office under Grant No. W911NF-04-1-0253 and from DARPA (optofluidic center) under Grant No. HR0011-04-1-0032. Support from the Center for Nanoscale Systems (CNS) at Harvard University is also gratefully acknowledged. Harvard-CNS is a member of the National Nanotechnology Infrastructure Network (NNIN).

¹A. A. Kosterev and F. K. Tittel, IEEE J. Quantum Electron. **38**, 582 (2002).

²D. D. Nelson, J. H. Shorter, J. B. McManus, and M. S. Zahniser, Appl. Phys. B: Lasers Opt. **75**, 343 (2002).

³R. Maulini, S. Yarekha, J. M. Bulliard, M. Giovannini, and J. Faist, Opt. Lett. **30**, 2584 (2005).

⁴J. S. Yu, S. Slivken, S. R. Darvish, A. Evans, G. Gokden, and M. Razeghi, Appl. Phys. Lett. **87**, 041104 (2005).

⁵A. Evans, J. S. Yu, S. Slivken, and M. Razeghi, Appl. Phys. Lett. **85**, 2166 (2004).

⁶A. Evans, J. S. Yu, J. David, L. Doris, K. Mi, S. Slivken, and M. Razeghi, Appl. Phys. Lett. **84**, 314 (2004).

⁷M. Troccoli, S. Corzine, D. Bour, J. Zhu, O. Assayag, L. Diehl, B. G. Lee, G. Höfler, and F. Capasso, Electron. Lett. **41**, 1059 (2005).

⁸D. Bour, M. Troccoli, F. Capasso, S. Corzine, A. Tandon, D. Mars, and G. Höfler, J. Cryst. Growth **272**, 526 (2004).

⁹M. Troccoli, D. Bour, S. Corzine, G. Höfler, A. Tandon, D. Mars, D. J. Smith, L. Diehl, and F. Capasso, Appl. Phys. Lett. **85**, 5842 (2004).

¹⁰D. Hofstetter, M. Beck, T. Aellen, J. Faist, U. Oesterle, M. Ilegems, E. Gini, and H. Melchior, Appl. Phys. Lett. **78**, 1964 (2001).

¹¹W. W. Bewley, J. R. Lindle, C. Soo Kim, I. Vurgaftman, J. R. Meyer, A. J. Evans, J. Su Yu, S. Slivken, and M. Razeghi, IEEE J. Quantum Electron. **41**, 833 (2005).

¹²S. Slivken, J. S. Yu, A. Evans, J. David, L. Doris, and M. Razeghi, IEEE Photon. Technol. Lett. **16**, 744 (2004).